ADVANCED MATERIALS

Fabrication of Anodic-Alumina Films with Custom-Designed Arrays of Nanochannels**

By *Nai-Wei Liu*, *Anindya Datta*, *Chih-Yi Liu*, *Cheng-Yi Peng*, *Huai-Hsien Wang*, and *Yuh-Lin Wang**

Among the strategies for growing one-dimensional nanostructures such as nanotubes and nanowires, a very viable approach is deposition of the desired material into a template with arrays of well-aligned nanochannels.[1–7] A competitive template with such characteristics is the porous anodic aluminum oxide (AAO) film, whose nanochannels can even laterally self-organize into hexagonally close-packed (hcp) domains exhibiting short-range order provided it is grown under specific anodization conditions.[8,9] It has been demonstrated that the range of the order can be further extended by several orders of magnitude using lithographic-guiding techniques,[4,10–12] and that the pore size distributions of such guided arrays are much narrower than those of the self-organized ones. The successful fabrication of such long-range-ordered nanochannel arrays, hereafter referred to simply as ordered arrays, has not only broadened the potential applications of AAO films but also opened possibilities for the fabrication of arrays of nanostructures arranged according to a custom-designed geometry. For example, one can envision an array with only part of it covered by nanodots or nanowires while the rest of the surface area remains empty. Depending on its geometry, such an array, with designed optical and electronic properties, could be used as a photonic crystal and/or a waveguide.[13–16] One of the viable approaches for fabricating such a custom-designed array is to grow the desired material into a template with a partially closed nanochannel array. Herein, we demonstrate a focused ion beam (FIB) direct-write lithographic method for selectively closing part of the channels of an ordered array on an AAO film in order to create a custom-designed nanochannel array. The initial ordered arrays were fabricated by FIB lithographic guiding techniques where the closure of the nanochannels within a certain area was achieved by raster scanning the FIB over the area, thus directly bombarding the AAO film. The successful fabrication of such a template with custom-designed nanochannel arrays opens up numerous possibilities for the creation of nanowire or nanodot arrays with desired geometric patterns.

The fabrication process always starts from growing an ordered array by anodizing a finely polished aluminum sample that has been patterned with a guiding lattice on its surface. The lattice is a two-dimensional array of hcp concave pits created by FIB direct-write lithography. An ordered array is achieved when the lattice constant of the guiding lattice is carefully matched with the electrolyte and anodization voltage.[17] For the present work, we set the lattice constant, and therefore the spacing, of the ordered array to be 100 nm, and grew the nanochannels to a typical aspect ratio of larger than ≈ 50. Figure 1a shows a micrograph of a typical ordered array on an AAO film taken by scanning with a 50 keV gallium FIB with a beam current of 1.1 pA and a diameter of ≈ 10 nm over the sample while collecting the secondary electron signal to provide the image contrast.[18,19] Using the digital raster scan (1024 pixels × 1024 pixels) and bitmap-controlled beam-blanking functions of the FIB, part of the nanochannels could be selectively closed by scanning the beam over the desired area under normal incidence, as shown by the schematic in Figure 1b. Examples of partially and completely closed nanochannels are shown in the FIB images in Figures 1c,d, respectively.

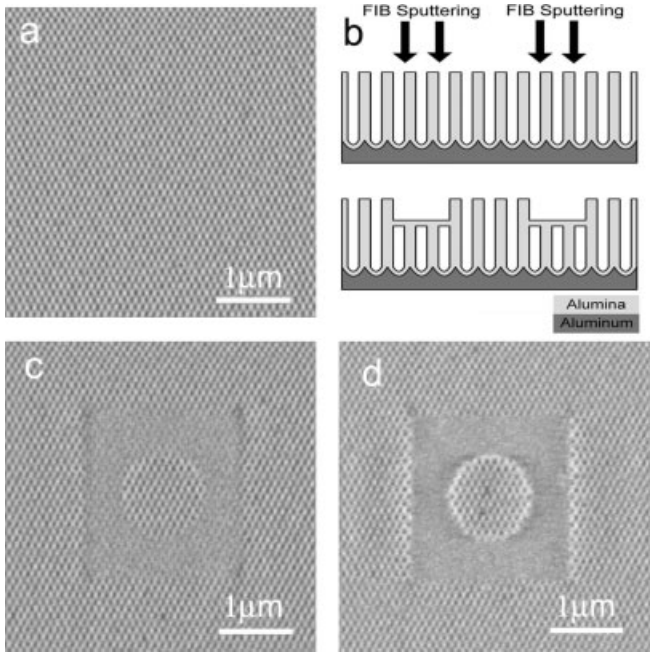

Figure 1. a) FIB image of an ordered nanochannel array on an AAO film before bombardment. b) Schematic diagram showing the process for selectively closing part of nanochannels in an array. Array after being bombarded by a dose of c) 2×10^{15} ions cm^{-2} and d) 5×10^{15} ions cm^{-2}, producing partially (c) and completely (d) closed nanochannels.

[*] Prof. Y.-L. Wang, N.-W. Liu, Dr. A. Datta,[+] Dr. C.-Y. Liu
Institute of Atomic and Molecular Sciences
Academia Sinica
P.O. Box 23-166, Taipei 106 (Taiwan)
E-mail: ylwang@pub.iams.sinica.edu.tw
N.-W. Liu
Department of Materials Science and Engineering
National Taiwan University
Taipei 106 (Taiwan)
Prof. Y.-L. Wang, C.-Y. Peng, H.-H. Wang
Department of Physics
National Taiwan University
Taipei 106 (Taiwan)
[+] Current address: Department of Physics, Netaji Nagar Day College, 170/436 N.S.C, Bose Road, Regent Estate, Kolkata 700 092, India.

[**] This work was partly funded by the National Science Council (NSC-93-2120-M-001-002) of Taiwan. C.-Y. Liu acknowledges the fellowship provided by Academia Sinica, Taiwan.

  DOI: 10.1002/adma.200400380

To quantify the morphological evolution of an ordered array as a function of ion dose and thus determine the dose needed for effective closing of the nanochannels, we employed an atomic force microscope (AFM) operated in contact mode to measure the root-mean-square (RMS) roughness of a 2 μm × 2 μm array after it was exposed to various ion doses. As shown in Figure 2, the surface roughness of the bombarded nanochannels becomes increasingly smooth with increasing ion dose. At a dose around 2×10^{15} ions cm^{-2}, the RMS surface roughness reached ≈ 2 nm, which is comparable to that of a freshly polished aluminum surface before anodization. The surface roughness remains essentially constant for arrays exposed to higher doses of ions. To ensure the complete closure of the nanochannels, we chose an ion dose of 5×10^{15} ions cm^{-2} for fabricating the custom-designed arrays described below.

Since the AFM measurement of the surface topography can only be conducted ex situ, we invented a more convenient method based on FIB images taken in situ from an ion-bombarded area. The intensity of the peaks on the two-dimensional Fourier transformation of the FIB image is a function of the ion dose and decreases monotonically with increasing dose, as shown in Figure 2. By calibrating the intensity with the RMS roughness measured by the AFM, it is possible to have an in situ measurement of the surface morphology,

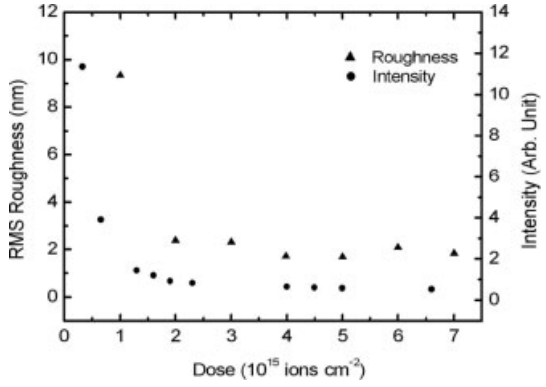

Figure 2. RMS surface roughness (measured by AFM) of the surface of an ordered array (▲) and maximum intensity of the peaks on the two-dimensional Fourier transformation of the corresponding FIB images (●) after different doses of FIB sputtering.

which can then be used as an in situ indicator for the closure of a nanochannel array.

To demonstrate the versatility of our fabrication process, several types of nanochannel arrays were fabricated. Figure 3a shows FIB images of a 1.5 μm × 1.5 μm array surrounded by closed nanochannels. Figure 3b exhibits an FIB image of one-quarter of an annular array surrounded by closed nanochannels. Such an array can be used, for example, as a photonic-crystal 90° bending waveguide. The linear array shown in Figure 3c demonstrates the precision of the fabrication process in one of the directions. The single-nanochannel AFM image

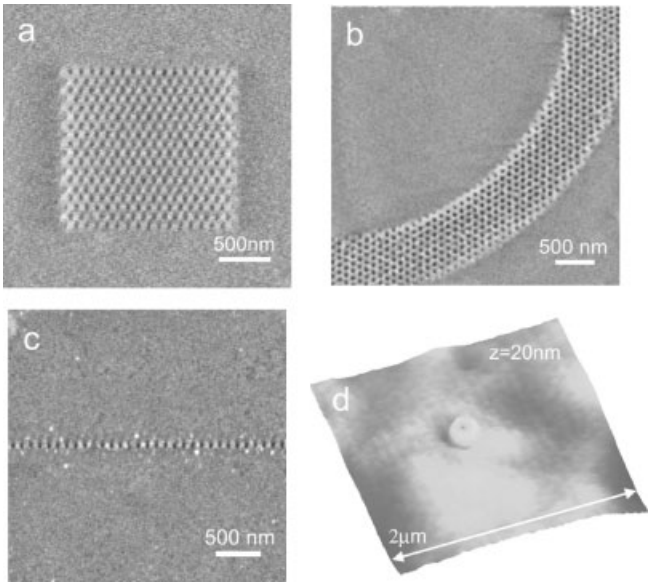

Figure 3. FIB images of a) a square array, b) one-quarter of an annular array, and c) a linear array. d) An AFM image of a single isolated nanochannel surrounded by closed nanochannels.

in Figure 3d shows the ultimate spatial resolution of the technique to be smaller than ≈ 50 nm, the pore diameter of the nanochannels used in this study. Note that the edge definition of an ion-bombarded area with closed nanochannels is as small as ≈ 20 nm. This limitation in the spatial resolution is certainly not intrinsic to the FIB-sputtering method. Since the diameter of the FIB is ≈ 10 nm, it is well within our reach to have much better resolution, provided that an ordered nanochannel array with smaller channel spacing could be fabricated.

To a great extent, the successful closure of nanochannels on specific positions of an array relies on its long-range order and size uniformity, which are not available in self-organized or ordinary random arrays of nanochannels on AAO films. The order and uniformity allow us to scan the FIB over an area outside the region of interest to acquire an image, and then extrapolate the coordinates to precisely determine the positions of the nanochannels to be closed. In comparison, closing specific channels on AAO films with either self-organized or ordinary random nanochannel arrays always requires the acquisition of an image to determine coordinates. Since the typical dose delivered to an area of 5 μm × 5 μm after one high-resolution imaging scan is around 5×10^{14} ions cm^{-2}, significant perturbation of the morphology of nanochannels could occur unintentionally during an imaging scan.

In the case where the closing of nanochannels in an entire area rather than specific channels is the main concern, it is not necessary to resort to the use of an ordered array. One can simply use a self-organized array. However, such a practice would require a minor modification of the channel-closing process described previously. Figure 4a shows the image of a boundary area between an ordered and a self-organized array after exposing to a dose of 5×10^{15} ions cm^{-2}. The nanochan-

ADVANCED MATERIALS

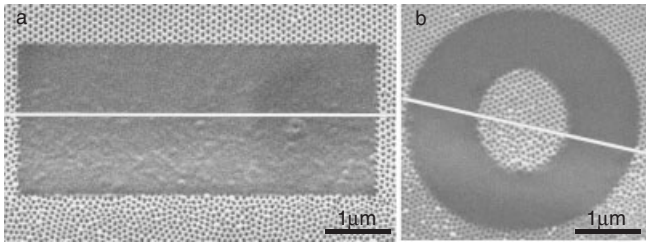

Figure 4. FIB images of two areas located on the boundary between an ordered and self-organized nanochannel array after exposing to a dose of a) 5×10^{15} ions cm^{-2} and b) 3×10^{16} ions cm^{-2}. The white lines indicate the positions of the boundaries.

nels on the ordered area are completely closed and its surface morphology is very flat, whereas the surface of the self-organized area is rough and covered by random, hole-like defects. Figure 4b shows the image of a boundary area between an ordered and a self-organized array in a ring pattern after exposing to a higher dose of 3×10^{16} ions cm^{-2}. At this dosage, the surfaces of both the ordered and self-organized array appear smooth. These measurements indicate that the ion dose required for closing the nanochannels of a self-organized array is higher than that for an ordered array.

To shed some light on the mechanism of channel closing induced by FIB bombardment, the cross-sections of some bombarded and neighboring pristine nanochannels were examined by scanning electron microscopy (SEM). As shown in Figure 5a, the bombarded nanochannels are capped by a $\approx$20 nm thick layer of material after exposing to a dose of 1×10^{16} ions cm^{-2}. The length of the nanochannels indeed becomes shorter after the bombardment, and the capping layer maintains its dynamical-equilibrium thickness (Fig. 5b) for ion doses as high as 1×10^{18} ions cm^{-2}. Since the capping layer is continuously sputtered away during the ion bombardment, the material must be supplied from either implanted gallium or residual gas in the FIB chamber (base pressure 1×10^{-6} Pa) or the wall of the nanochannels in order to maintain its equilibrium thickness. To differentiate between these two likely

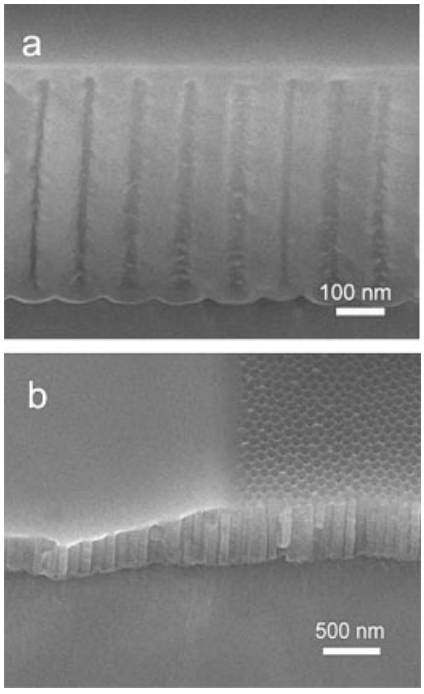

Figure 5. Cross-sectional SEM images of a) nanochannels exposed to a dose of 1×10^{16} ions cm^{-2}, and b) the boundary of the region between pristine and heavily bombarded (1×10^{18} ions cm^{-2}) nanochannel arrays.

supply sources, the composition of the AAO film was examined by energy dispersive spectrometry (EDS). Figure 6a shows that a pristine nanochannel array on an AAO film contains only aluminum and oxygen. Figure 6b indicates that the FIB-exposed area, as shown in the insets, contains $\approx$1–2 % atomic concentration of gallium. Such a low concentration of gallium rules out its possibility as a prime source of material supply to the capping layer, while the lack of other elements in the EDS spectrum helps to reduce the possibility that ion-induced contaminants are the main cause for the closing of the nanochannels.

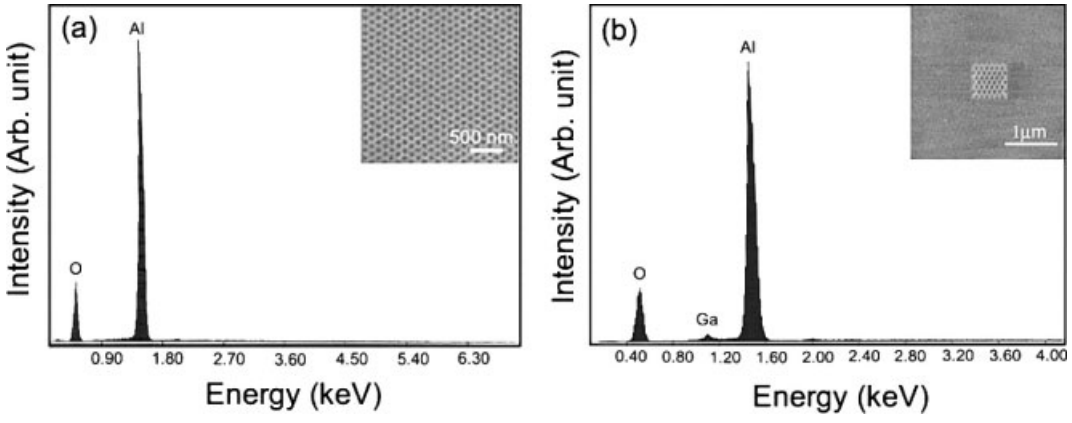

Figure 6. EDS spectra of a) a pristine AAO nanochannel array, and b) an array partially closed by FIB sputtering. The insets show the FIB images of the corresponding areas from which the spectra were taken.

One of the possible mechanisms for ion-induced closing of the nanochannels is the swelling of the AAO film caused by gallium implantation. Such radiation-induced swelling of material is well-documented; however, it is unlikely to be the key factor because the nanochannels have pore radii of ≈ 20 nm and wall thicknesses of ≈ 30 nm, and the swelling factor needed for completely closing the nanochannels would be as large as ≈ 67 %. In comparison with the ≈ 2% swelling of silicon caused by 50 keV gallium-ion bombardment,[20] such a hypothetical swelling factor of alumina appears unrealistic. More likely, some other mechanisms are responsible for the ion-induced closing. For example, redeposition of sputtered material onto the sidewalls of the pore openings could be among the contributors to the initial phase of the channel closing. Since the longitudinal range and longitudinal straggling of 50 keV gallium in alumina is calculated to be as large as 46 nm and 15 nm respectively,[21] material could be sputtered from the sidewall (≈ 30 nm) of a nanochannel even after it is covered by the capping layer (≈ 20 nm). Therefore, the material ejected from the buried sidewall could be redeposited onto the bottom of the capping layer, replenishing the material sputtered from its top surface. Another possible mechanism is the ion-induced lateral migration and/or diffusion of material, which could also, in principle, build up the initial capping layer and maintain its equilibrium thickness afterwards. Apparently, more detailed studies are needed to help clarify the mechanisms responsible for this fascinating phenomenon of ion-induced closing of nanochannels on an AAO film.

In conclusion, we have employed FIB to selectively close nanochannels of an ordered array on an AAO film, thereby fabricating special templates with nanochannels arranged in certain custom-designed geometries. The closing of the nanochannels can be monitored in situ by FIB imaging during the closing process. The capability to fabricate square, linear, and annular arrays is demonstrated, and is extended to the extreme case where an isolated individual nanochannel is closed. This technique for creating a custom-designed array of nanochannels with a high aspect ratio can be used to fabricate specially designed filters and templates, upon which various nanocomposites and nanodevices could be built. The mechanism for the ion-induced closing of nanochannels on AAO remains to be understood.

Experimental

High-purity annealed aluminum samples were prepared by electropolishing in a mixed solution of 50 % $HClO_4$ and C_2H_5OH (1:5 v/v) at 5 °C under constant stirring until the root-mean-square roughness of a 10 μm × 10 μm surface area was ≈ 1 nm, as measured by contact-mode atomic force microscopy. A 50 keV gallium focused ion beam with a diameter of ≈ 10 nm and beam current of 1.1 pA was employed to create arrays of hexagonal close-packed single-pixel concave pits on polished, polycrystalline-aluminum surfaces. The dwell time was 9 ms pixel^{-1}, and the lattice constant of the array was set to 100 nm in order to match the anodization electrolyte and voltage used in the experiments. The anodization was carried out in 0.3 M oxalic acid solution at 3 °C with a constant voltage of 40 V. After anodization, the nanochannels were opened in a 5 wt.-% solution of phosphoric acid (H_3PO_4) at room temperature. To create a freestanding anodic aluminum oxide film, the remaining aluminum substrate was removed by a saturated $HgCl_2$ solution. If needed, the barrier layer, i.e., an oxide layer on the bottom of the nanochannels, was etched by a 5 wt.-% H_3PO_4 solution, also at room temperature, for 40 min.

Received: March 12, 2004
Final version: July 26, 2004

[1] Y. Li, G. W. Meng, L. D. Zhang, F. Phillipp, *Appl. Phys. Lett.* **2000**, *76*, 2011.
[2] T. G. Tsai, K. J. Chao, X. J. Guo, S. L. Sung, C. N. Wu, Y. L. Wang, H. C. Shih, *Adv. Mater.* **1997**, *9*, 1154.
[3] J. S. Suh, J. S. Lee, *Appl. Phys. Lett.* **1999**, *75*, 2047.
[4] H. Masuda, M. Satoh, *Jpn. J. Appl. Phys., Part 2* **1996**, *35*, L126.
[5] M. Nakao, S. Oku, T. Tamamura, Y. Yasui, H. Masuda, *Jpn. J. Appl. Phys., Part 1* **1999**, *38*, 1052.
[6] H. Masuda, K. Fukuda, *Science* **1995**, *268*, 1466.
[7] J. Li, C. Papadopoulos, J. Xu, *Nature* **1999**, *402*, 253.
[8] H. Masuda, F. Hasegwa, S. Ono, *J. Electrochem. Soc.* **1997**, *144*, L127.
[9] A. P. Li, F. Müller, A. Birner, K. Nielsch, U. Gösele, *J. Appl. Phys.* **1998**, *84*, 6023.
[10] H. Masuda, H. Yamada, M. Satoh, H. Asoh, *Appl. Phys. Lett.* **1997**, *71*, 2770.
[11] C. Y. Liu, A. Datta, Y. L. Wang, *Appl. Phys. Lett.* **2001**, *78*, 120.
[12] N. W. Liu, A. Datta, C. Y. Liu, Y. L. Wang, *Appl. Phys. Lett.* **2003**, *82*, 1281.
[13] J. Li, D. Stein, C. McMullan, D. Branton, M. J. Aziz, J. A. Golovchenko, *Nature* **2001**, *412*, 166.
[14] C. Zhou, M. R. Despande, M. A. Reed, *Appl. Phys. Lett.* **1997**, *71*, 611.
[15] D. C. Ralph, C. T. Black, M. Tinkham, *Phys. Rev. Lett.* **1995**, *74*, 3241.
[16] M. M. Deshmukh, D. C. Ralph, M. Thomas, J. Silcox, *Appl. Phys. Lett.* **1999**, *75*, 1631.
[17] C. Y. Liu, A. Datta, N. W. Liu, C. Y. Peng, Y. L. Wang, *Appl. Phys. Lett.* **2004**, *84*, 2509.
[18] P. H. La Marche, R. Levi-Setti, Y. L. Wang, *J. Vac. Sci. Technol., B: Microelectron. Process. Phenom.* **1983**, *B1*, 1056.
[19] Y. L. Wang, Z. Shao, in *Advances in Electronics and Electron Physics* (Ed: P. W. Hawkes), Vol. 81, Academic, Boston, MA **1991**, p. 177.
[20] J. B. Wang, A. Datta, Y. L. Wang, *Appl. Surf. Sci.* **1998**, *135*, 129.
[21] J. F. Zeigler, J. P. Biersack, SRIM (TRIM 90) Simulation Package (1995), IBM Research, 28-024 Yorktown, NY 10598.

Single-Catalyst Confined Growth of ZnS/Si Composite Nanowires**

By *Jinhua Zhan*,* *Yoshio Bando*, *Junqing Hu*, *Takashi Sekiguchi*, and *Dmitri Golberg*

One-dimensional (1D) nanomaterials have attracted considerable attention due to their potential application as building blocks in nanoscale circuits and optoelectronic devices.[1–3] The

[*] Dr. J. Zhan, Prof. Y. Bando, Dr. J. Hu, Dr. T. Sekiguchi, Dr. D. Golberg
Advanced Materials Laboratory and Nanomaterials Laboratory
National Institute for Materials Science
Namiki 1-1, Tsukuba, Ibaraki 305-0044 (Japan)
E-mail: ZHAN.Jinhua@nims.go.jp

[**] Supporting Information is available online from Wiley InterScience or from the author.

DOI: 10.1002/adma.200400585